Optically active defect states and valley depolarization in monolayer MoS_2 induced by high-energy electron beam irradiation

Anagha Gopinath[1] Faiha Mujeeb[2] Subhabrata Dhar[2] Jyoti Mohanty[1]

1. Nanomagnetism and Microscopy Laboratory, Department of Physics, Indian Institute of Technology Hyderabad, Kandi, Sangareddy, Telangana, India

2. Department of Physics, Indian Institute of Technology Bombay, Powai, Mumbai, India

1.

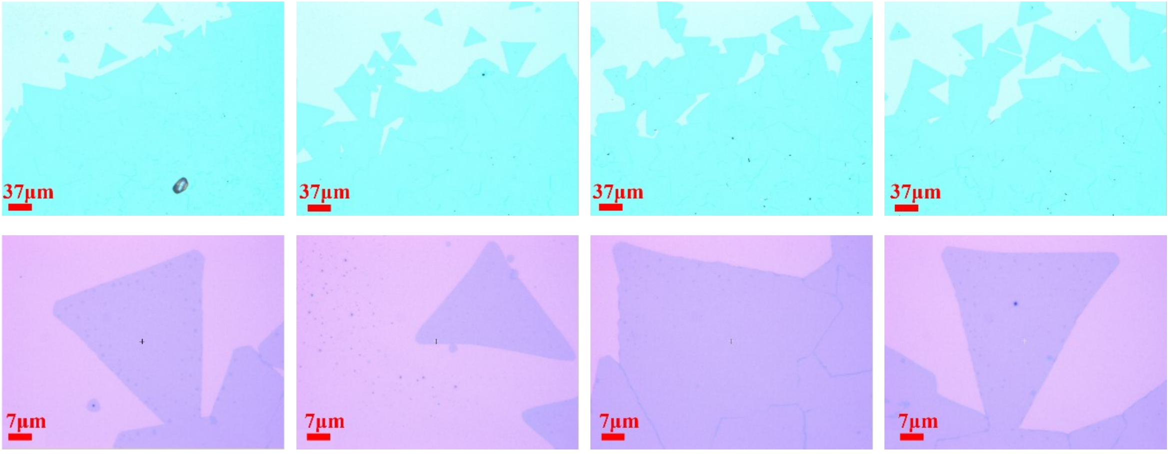

Figure S.1(a): Optical microscopy images of as-grown sample

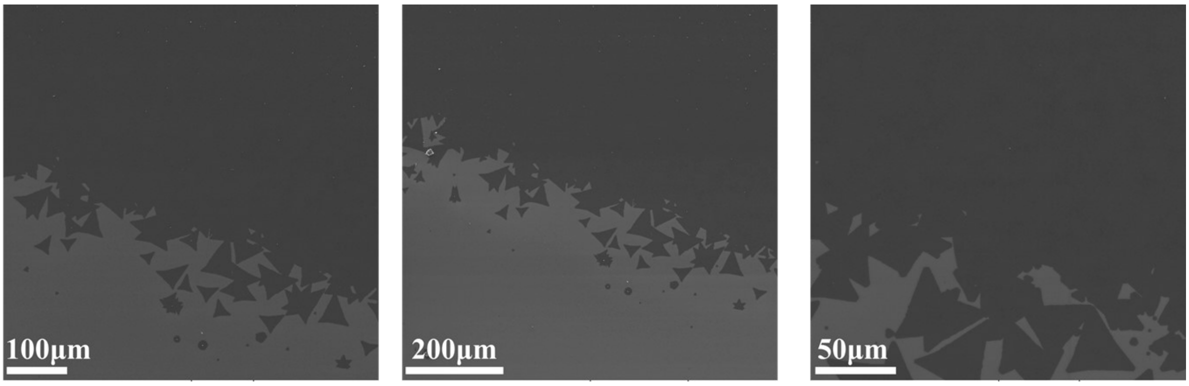

Figure S.1(b): Scanning electron microscopy images of as-grown sample

2.

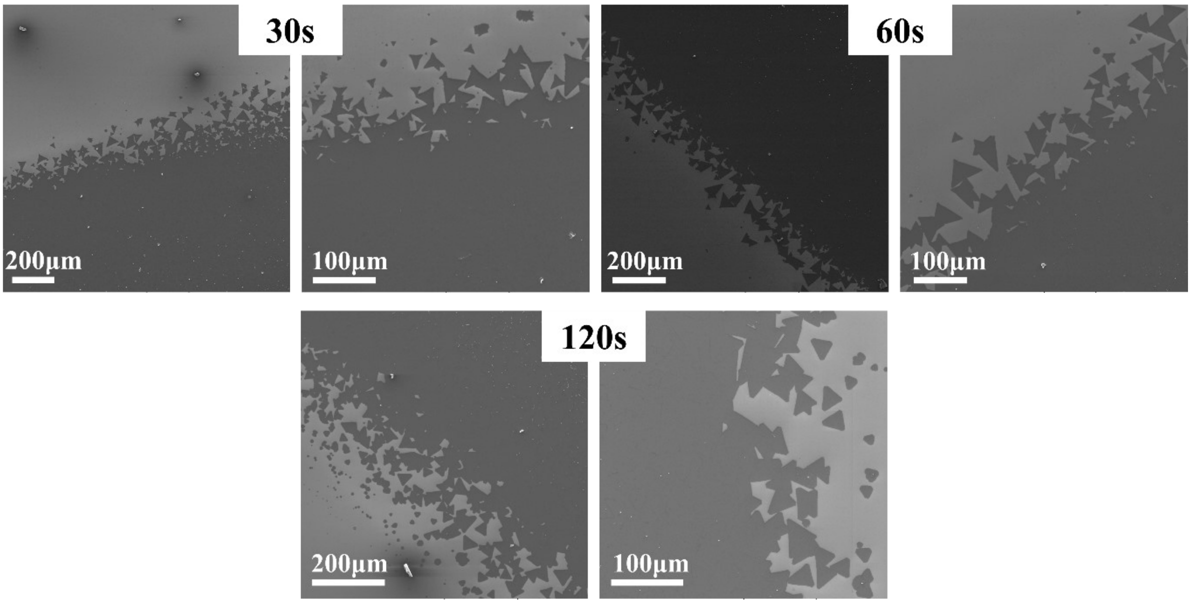

Figure S.2: Scanning electron microscopy images of irradiated samples. The spherical particles observed on the sample surface are precursor residues from the chemical vapor deposition process.

3.

Irradiation Time	S $2p_{3/2}$ (eV)	S $2p_{1/2}$ (eV)	Mo $3d_{5/2}$ (eV)	Mo $3d_{3/2}$ (eV)
As-grown	162.64728± 0.00751	163.81529± 0.01518	229.82746± 0.002	232.9866± 0.00352
30s	162.63956± 0.00966	163.83626± 0.02179	229.8051± 0.00203	232.93306± 0.00991
60s	163.00693± 0.00427	164.25543± 0.00728	230.07758± 0.00082633	233.31246± 0.00213
120s	162.91879± 0.00164	164.09103± 0.00323	230.09569± 0.00375	233.26901± 0.0114

Table S.1: Extracted fitting parameters from XPS spectra

4.

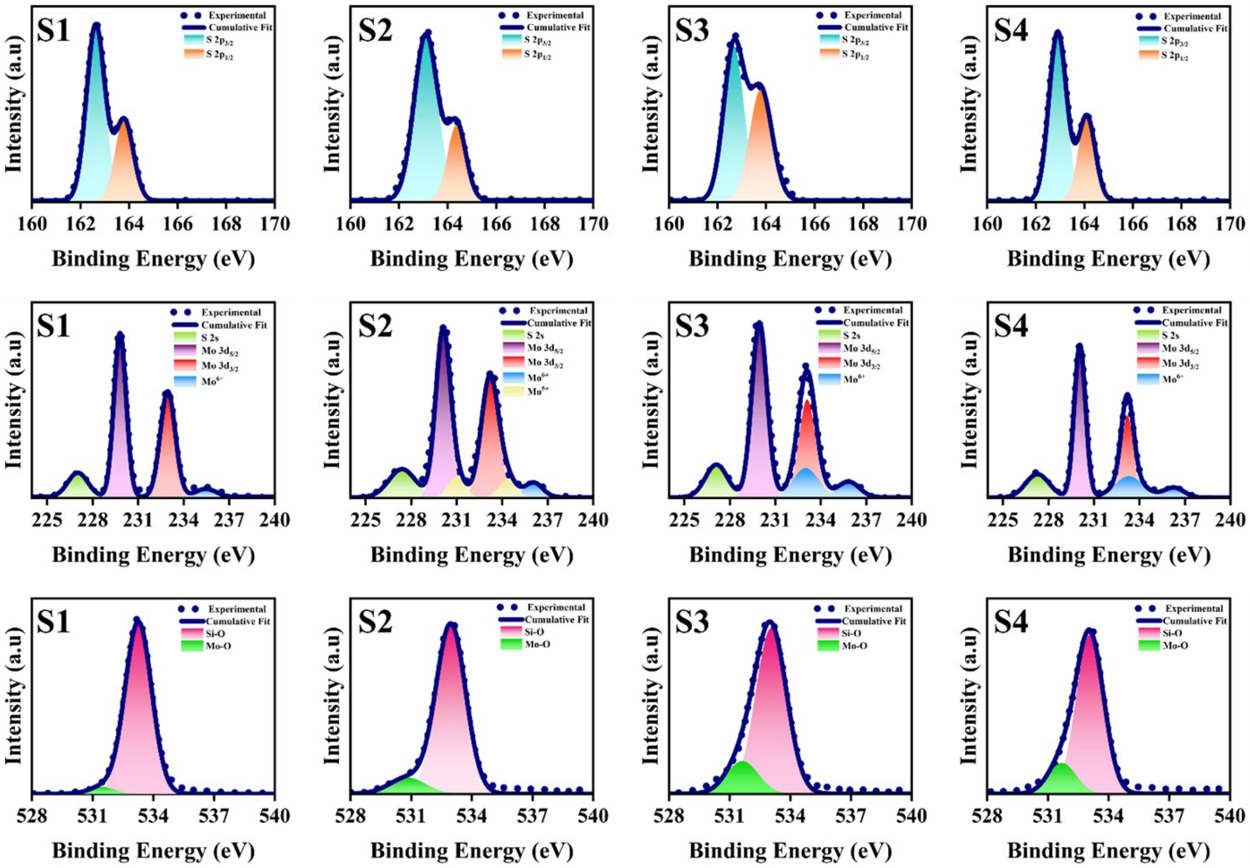

Figure S.3: XPS spectra of S-2p, Mo-3d and O-1s . S1 corresponds to the as-grown monolayer MoS_2 sample. S2, S3, and S4 represent samples irradiated with ~1MeV electron beam for 30s, 60s, and 120s, delivering fluences of 3.6 × 10^8 electrons/cm^2, 7.2 × 10^8 electrons/cm^2, and 1.44 × 10^9 electrons/cm^2, respectively.

5.

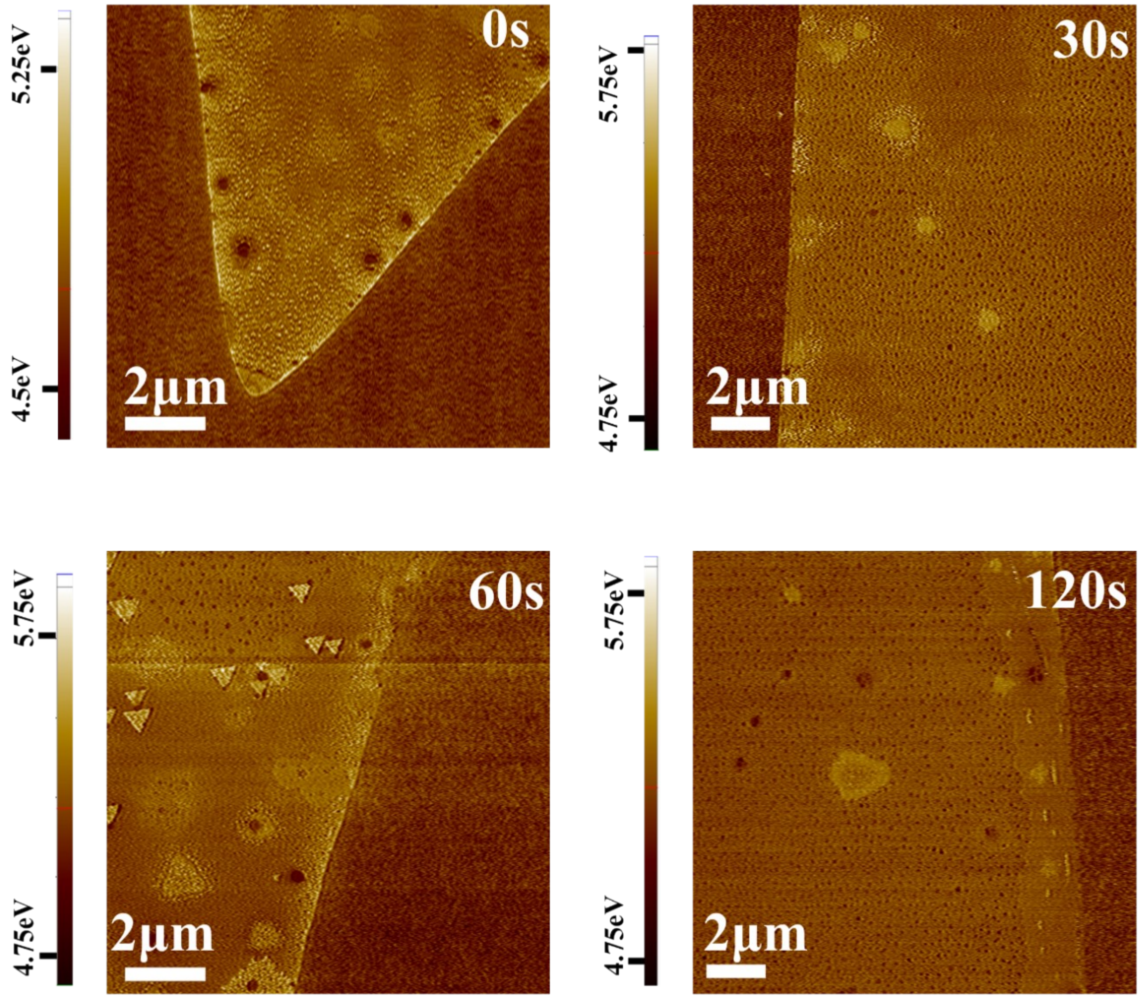

Figure S.4: Workfunction mapping of as-grown and irradiated samples obtained from Kelvin Probe force microscopy analysis

6.

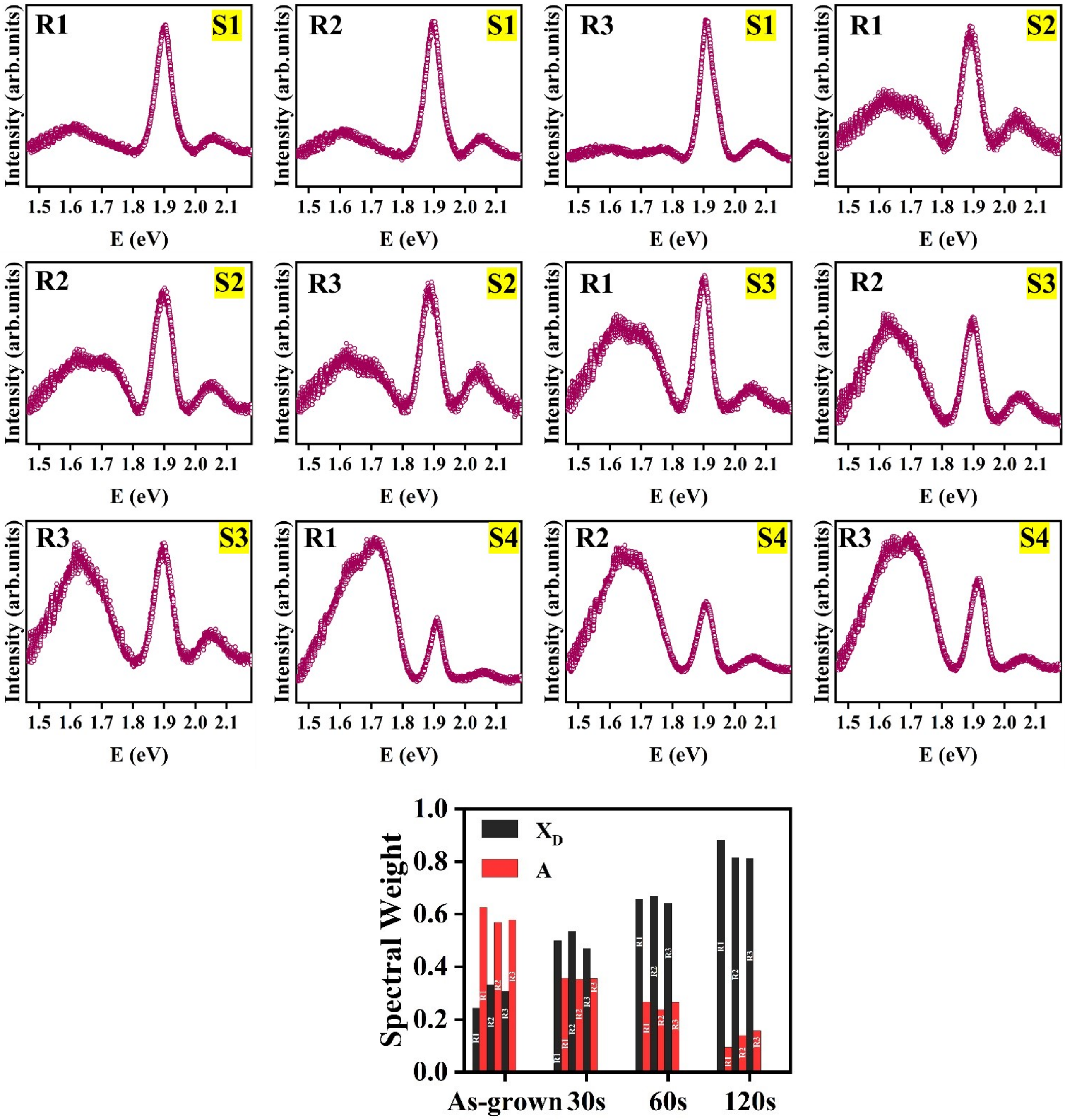

Figure S.5: Photoluminescence spectra acquired at 85K from different regions (labelled as R1, R2 and R3) of samples S1(as-grown), S2(30s irradiated), S3(60s irradiated), and S4 (120s irradiated). The corresponding spectral weight is also shown, indicating the consistent response of MoS_2 to irradiation. Bound exciton (X_D) and A-exciton emissions are indicated in black and red, respectively.

7.

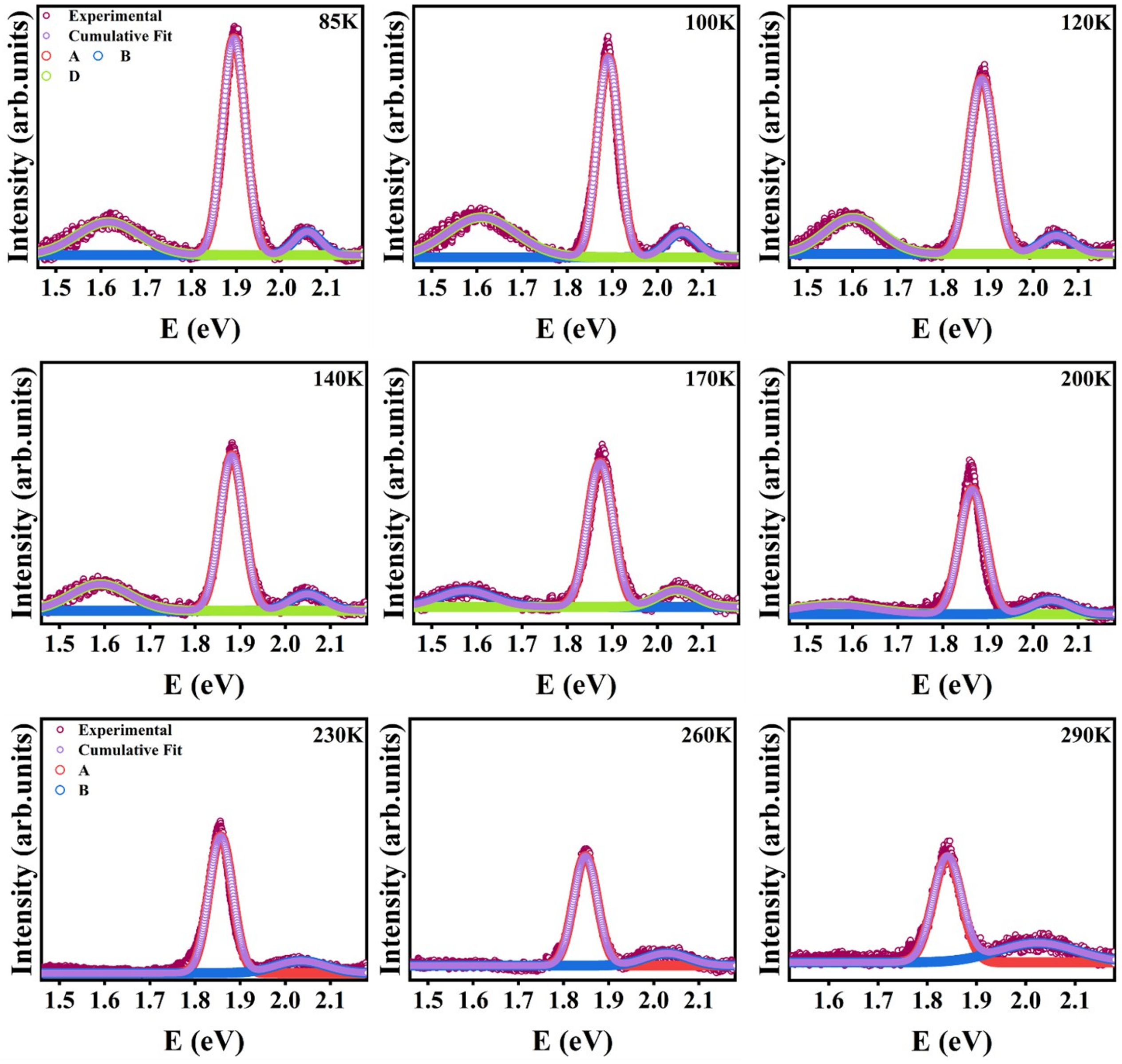

Figure S.6(a): Temperature-dependent photoluminescence (PL) spectra of as-grown MoS_2 (sample S1). PL spectra measured between 85–290 K (temperature shown in each panel) are fitted using Gaussian deconvolution. The Spectra is dominated by A exciton, B exciton, and a defect-related emission D at lower energy. With increasing temperature, the A and B exciton redshift and the defect emission is quenched, leaving primarily the A and B excitonic peaks above ~230 K.

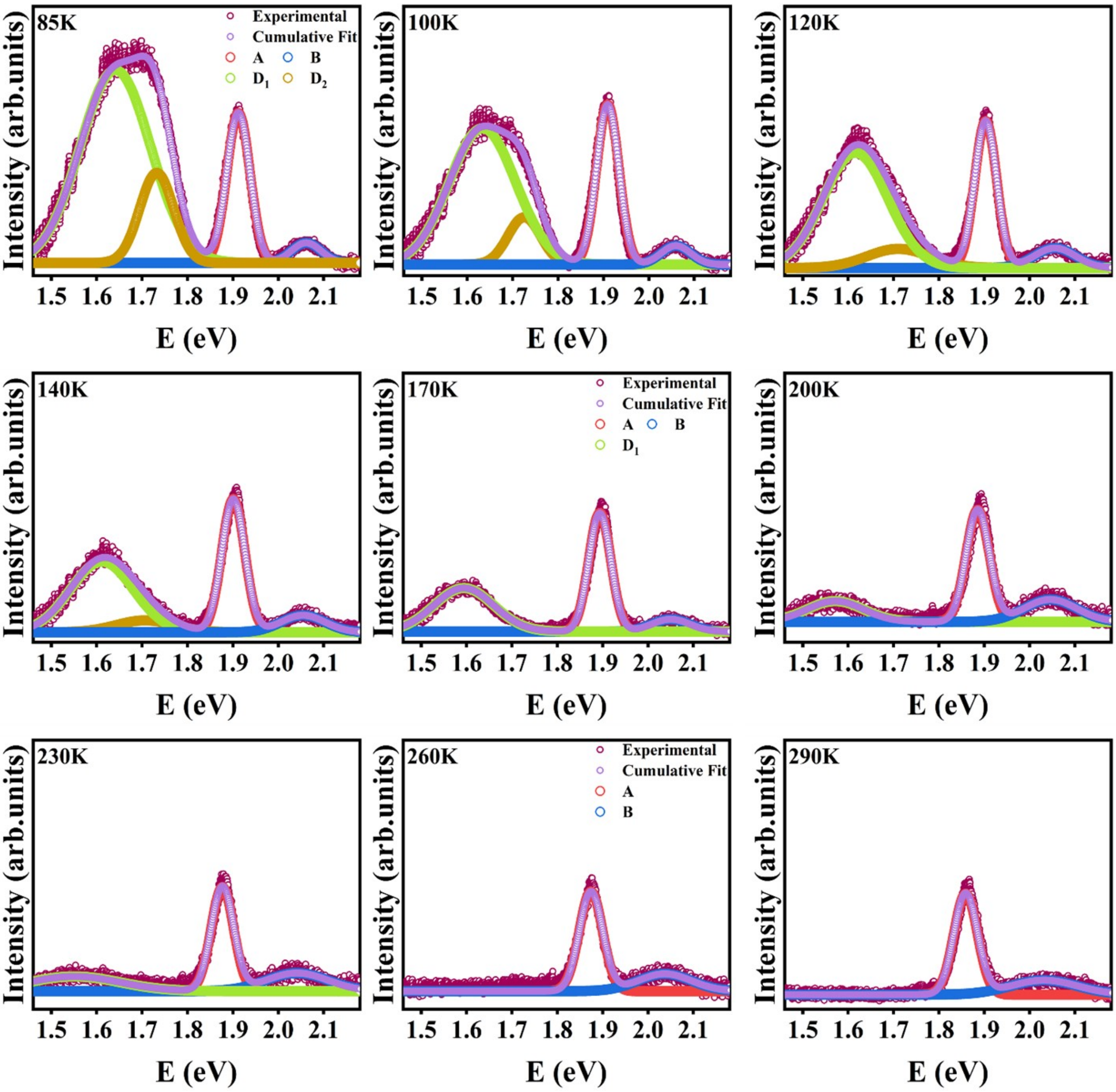

Figure S.6(b): Temperature-dependent photoluminescence (PL) spectra of electron-beam irradiated MoS_2 at a fluence of 1.44×10^9 electrons/cm^2 (Sample S4). PL spectra measured between 85–290 K (temperature shown in each panel) are fitted using Gaussian deconvolution. The Spectra is dominated by the A exciton, the B exciton, and the defect-related emissions D_1 and D_2 at lower energy. The defect emissions are quenched at higher temperatures, leaving primarily the A and B excitonic peaks above ~230 K.

8.

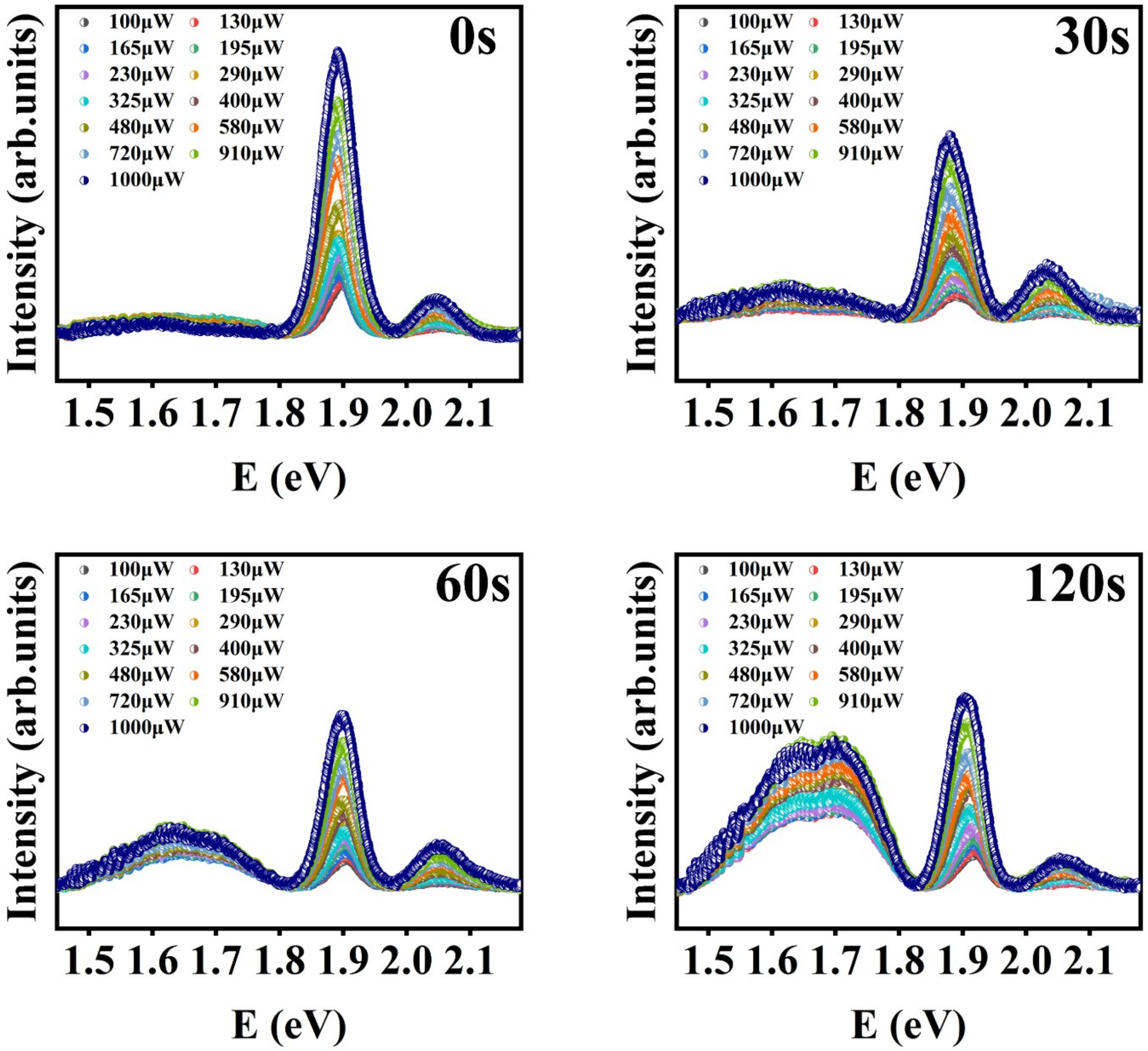

Figure S.7: Power-dependent photoluminescence (PL) spectra of as-grown and irradiated samples. PL spectra were measured at excitation powers ranging from 100 μW to 1000 μW.

9.

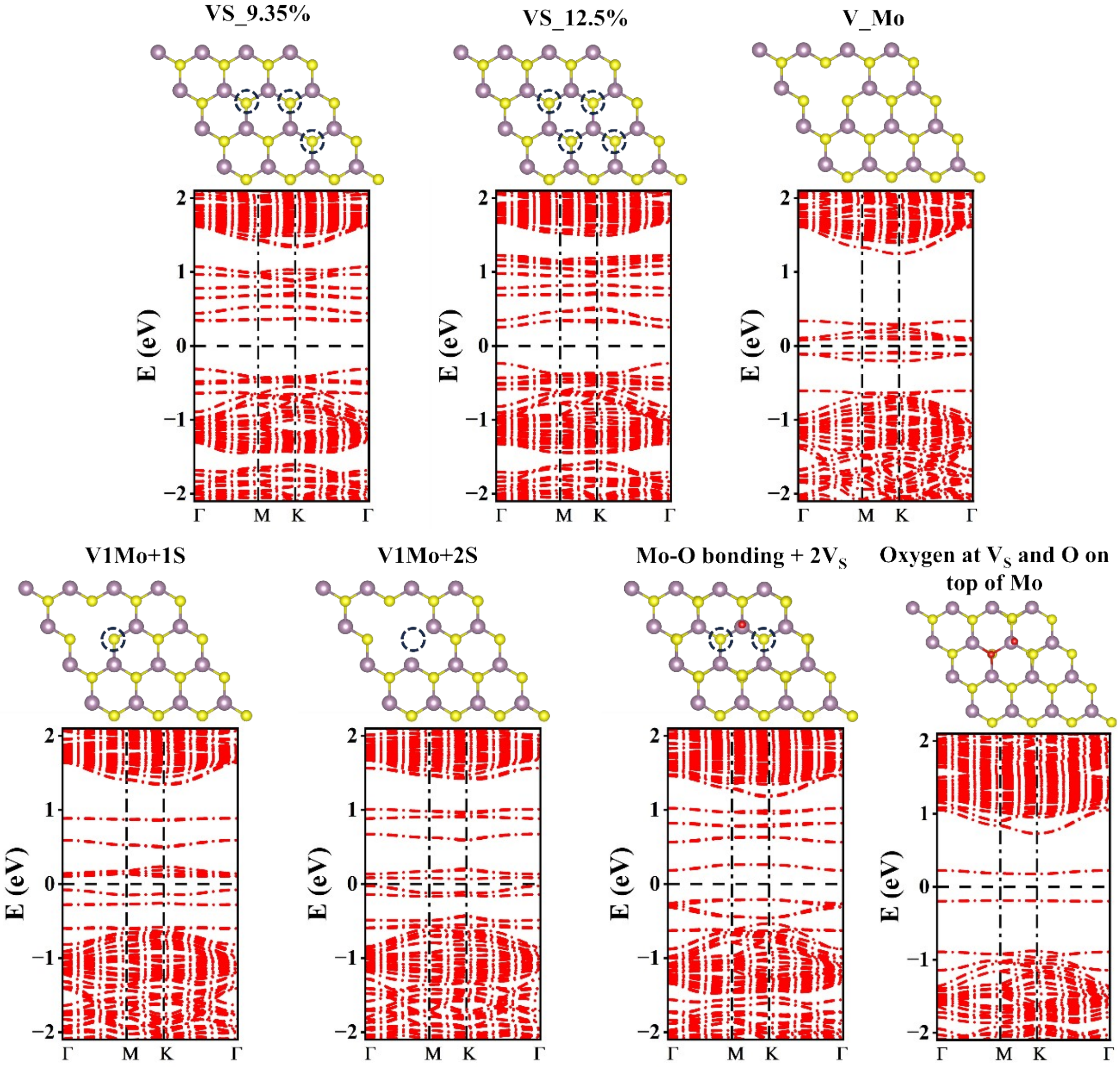

Figure S.8: Electronic band-structure of monolayer MoS_2 with various defect configurations. The blue dotted circles indicate the sulfur vacancy sites. Increased defect concentration leads to more mid-gap states within the band-gap.

10.

Configurations	**$E_{\Gamma\text{-}K}$ (eV)**	**Configurations**	**$E_{\Gamma\text{-}K}$ (eV)**
Pristine	0.4917	$1O_2$ physisorption+V_{1S}	0.3514
V_{1S}	0.4195	$2O_2$ physisorption	0.3539
V_{2S}	0.3492	$1O_2$ physisorption+$1O_2$ bonding	0.1632
$1O_2$ bonding+V_{1S}	0.2067	Mo-O-Mo+V_{1S}	0.4613
$2O_2$ bonding	0.202	Mo-O bonding+V_{1S}	0.3313

Table S.2: Calculated energy separation between Γ and K points for the electronic band structures shown in the figure.8